

University of Groningen

Brilliant biophotonics

Wilts, Bodo Dirk

IMPORTANT NOTE: You are advised to consult the publisher's version (publisher's PDF) if you wish to cite from it. Please check the document version below.

Document Version

Publisher's PDF, also known as Version of record

Publication date:

2013

[Link to publication in University of Groningen/UMCG research database](#)

Citation for published version (APA):

Wilts, B. D. (2013). *Brilliant biophotonics: physical properties, pigmentary tuning & biological implications*. s.n.

Copyright

Other than for strictly personal use, it is not permitted to download or to forward/distribute the text or part of it without the consent of the author(s) and/or copyright holder(s), unless the work is under an open content license (like Creative Commons).

The publication may also be distributed here under the terms of Article 25fa of the Dutch Copyright Act, indicated by the "Taverne" license. More information can be found on the University of Groningen website: <https://www.rug.nl/library/open-access/self-archiving-pure/taverne-amendment>.

Take-down policy

If you believe that this document breaches copyright please contact us providing details, and we will remove access to the work immediately and investigate your claim.

Downloaded from the University of Groningen/UMCG research database (Pure): <http://www.rug.nl/research/portal>. For technical reasons the number of authors shown on this cover page is limited to 10 maximum.

CHAPTER 10

Brilliant camouflage – Photonic crystals in the diamond weevil, *Entimus imperialis*

ABSTRACT

The neotropical diamond weevil, *Entimus imperialis*, is marked by rows of brilliant spots on the overall black elytra. The spots are concave pits with intricate patterns of structural-coloured scales, consisting of large domains of three-dimensional photonic crystals that have a diamond-type structure. Reflectance spectra measured from individual scale domains perfectly match model spectra, calculated with anatomical data and finite-difference time-domain methods. The reflections of single domains are extremely directional (observed with a point source $< 5^\circ$), but the special arrangement of the scales in the concave pits significantly broadens the angular distribution of the reflections. The resulting virtually angle-independent green colouration of the weevil closely approximates the colour of a foliaceous background. While the close-distance colourful shininess of *E. imperialis* may facilitate intersexual recognition, the diffuse green reflectance of the elytra when seen at long-distance provides cryptic camouflage.

* This chapter has been published as
Wilts BD, Michielsen K, Kuipers J, De Raedt H and Stavenga DG.
Proceedings of the Royal Society B **279**: 2524-2530, 2012.

INTRODUCTION

Animal colouration is due to spectrally selective light reflections on the outer body parts [1,2]. The resulting colouration mostly serves a biological function in intra- and interspecific signalling [3,4], thus improving mating chances [5], but it can also be used for camouflage in the animal's native habitat [6-8]. Generally two types of colouration are recognised, pigmentary and structural. Pigmentary (or chemical) colouration occurs when pigments absorb incoherently scattered light in a restricted wavelength range. Structural (or physical) colouration is due to nanometre-sized structures with periodically changing refractive indices, causing coherent light scattering. Pigmentary colouration is by far the most common in the animal kingdom, but structural colouration is widely encountered as well, and not seldom structural colours are modified by spectrally filtering pigments [1,2,9].

If the structures causing the physical colours are regular with a periodicity in the order of the wavelength of visible light, the materials are referred to as photonic crystals [10]. One-dimensional photonic crystals consist of parallel thin film layers of alternating high and low refractive index materials, i.e. the well-known multilayers. They create the metallic and polarised reflections of, for example, the skin of cephalopods [9] and fish [11], the elytra of jewel beetles [12-15], scarabs [16,17] and the breast feathers of birds of paradise [18]. Two-dimensional photonic crystals, that is, structures with periodicity in two dimensions, underlie the colouration of peacock feathers [19,20]. Three-dimensional photonic crystals have been found in the scales of many weevils and beetles [1,21-24], but also in butterflies [25-28]. Quasi-ordered 3D photonic crystal structures, which are periodic in all three dimensions, although imperfect, have been identified in bird feathers [29] and in the scales of some coleopterans [30].

The colourations of the elytra of weevils and beetles are especially diverse [1,2]. Here we investigate the diamond weevil, *Entimus imperialis*, which is endemic to the Neotropical regions, especially south-west Brazil [31]. *E. imperialis* is a member of the monophyletic genus *Entimus* (Curculinoidea: Entiminae: Entimini). The relatively large weevils of this genus, with a 15-45 mm body length, have strikingly iridescent scales, immersed in pits on the weevil's elytra and legs (figure 1a). A unique property of the elytral scales of *E. imperialis* is the presence of extremely large, crystalline domains, which allows an in-depth analysis of their physical properties. In a previous study, we identified the domains to be single-network diamond-type photonic crystals [22]. Here we present reflectance spectra of single domains together with calculated reflectance spectra of the domains, based on their anatomical dimensions. We find that perfect matches of the experimental and computationally derived spectra can be obtained for appropriate orientations of the crystalline structure. We thus demonstrate, for the first time, that the optical properties of the weevil scales can be quantitatively understood.

Curiously, the scales are arranged inside concave pits. This leads to a drastic change in appearance of the animal when observed at long distance or from close-up. Measurement of the integral reflectance of the scale assembly in the elytral pits yielded spectra matching the spectrum of a green, foliaceous background, the weevil's natural habitat [32]. This suggests that the scale set is optimized for camouflage for distant predators. However, the concentration of the glittering scales in distinct pits causes a spotted patterning for observers at close range. The bright patterning may allow ready recognition for nearby conspecifics.

Animals

A specimen of the diamond weevil, *Entimus imperialis*, of the Coleoptera collection in the Natural History Museum Naturalis (Leiden, the Netherlands; curator J. Krikken), was photographed with a Canon EOS-30D camera. Extensive investigations were performed on a specimen obtained from Prof. J.-P. Vigneron (University of Namur, Belgium).

Modelling

The light scattering by single-network diamond photonic crystals was simulated for a number of differently oriented crystals with three-dimensional finite-difference time-domain (FDTD) calculations. We used TDME3D, a massively parallel Maxwell equation solver [6], as described in

Chapter 3.

RESULTS

Optical appearance of the diamond weevil scales

The diamond weevil, *E. imperialis*, has overall black elytra, which are marked by rows of yellow-green glittering spots (figure 1a,b). With only minor changes of the viewing angle, the shiny spots feature strikingly different colours, which give them a diamond-like appearance. The strong directionality of the reflections indicates that the origin of these local, vivid colours is structural [2,3].

A closer look at the elytral pits shows that the diamond-like spots are assemblies of highly directionally reflective scales covering the walls of concave pits in the elytra (figure 1b). Similar brilliant scales are also found on the thorax and the legs of the weevil (figure 1a; see also ref. [31]). Single wing scales have an elongated shape, with length 100 μm and width 50 μm . The scales consist of coloured domains, with colour ranging from turquoise to yellow-orange. Most scales feature a few (three to five) large domains (figure 1c); a minority of scales have only one domain.

The coloured domains, when observed with an epi-illumination microscope at high magnification, resolve into striped patterns with orientations depending on the colour of the domains (figure 1c, see also figure 2a of [22]). The striped, grating-like patterns with different orientations strongly suggested that the scale lumen contains differently ordered crystalline structures. In a separate study we identified the structures inside the scales by using a novel optical characterisation technique, namely hemispherical Brillouin zone imaging [22]. We found that the scale interior consists of an ordered, three-dimensional lattice of chitin, enveloped by an external cuticular cortex. The air-chitin assembly forms a three-dimensional single-network diamond photonic crystal with face-centred cubic lattice symmetry [22]. The scales have a chitin filling fraction of ~ 0.3 and a lattice constant 445 ± 10 nm (figure 1e).

Biological photonic crystals like that of the *Entimus* weevil have a low refractive index contrast (for air-chitin assemblies: 1.56) [35,36]. Consequently, the spatial direction and spectral distribution of the light reflected by the crystal depends on the orientation of the crystal with respect to the direction of illumination [6,10]. In other words, the different-coloured domains of the weevil's scales are due to differently oriented photonic crystals (figure 1b,c) [22].

¹ Materials and Methods are presented in more detail in **Chapters 2 and 3.**

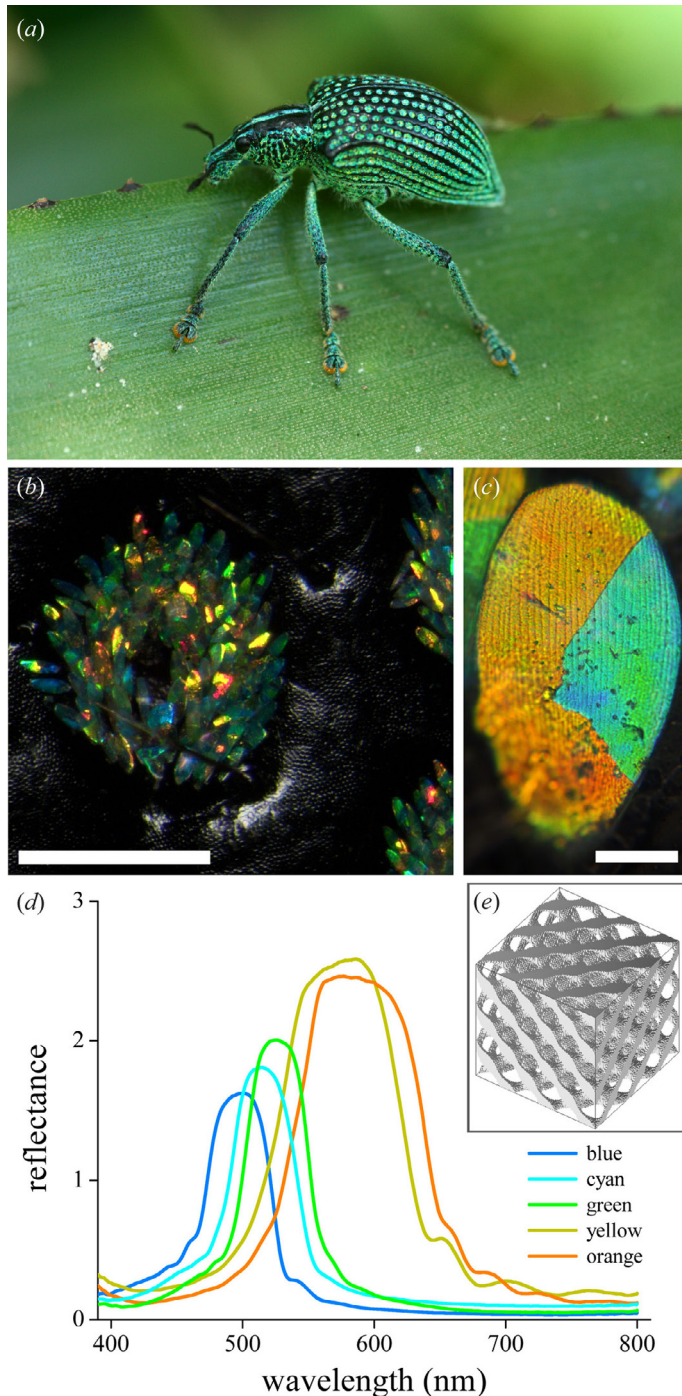


Figure 1. The diamond weevil, *Entimus imperialis*. (a) The intact animal with its black elytra studded with numerous yellow-green pits, sitting on a green leaf. (b) A single pit as seen in an epi-illumination microscope (bar: 0.5 mm). (c) A single scale with a few differently coloured domains (bar: 20 μm). (d) Reflectance spectra of single, differently coloured domains measured with a microspectrophotometer, applying white-light illumination at about normal incidence, with a white diffuser as a reference. (e) Rendered model of the single diamond photonic crystal found inside the scale lumen.

Reflectance spectra measured from single scale domains

To quantify the observed scale colours, we measured the reflectance spectra of single scale domains with a microspectrophotometer (MSP). This yielded a set of representative narrow-band reflectance spectra with half-width (FWHM - full width at half maximum) ~50-80 nm and peak wavelengths at ~480 nm (turquoise-blue), ~520 nm (cyan), ~540 nm (green), and between 560 nm to 610 nm (yellow-orange). The amplitude of the measured spectra increased with the peak wavelength (figure 1d).

Orientations of single domains and modelling of the photonic response

For a quantitative understanding of the photonic response of a single domain, its crystal orientation inside the scale has to be known. We therefore performed TEM on single scales. Figure 2 (left column) shows the most commonly encountered crystal orientations in single scale cross-sections. We compared the TEM images, obtained from ~70 nm thick sections, with computer-generated, projections modelled by level surfaces equivalent to 70 nm thick sections of single diamond photonic crystal structures. We therefore rotated the modelled sections stepwise until the computationally created projection matched the pattern of the experimentally obtained TEM sections (figure 2, right column). Matching images could only be obtained for a single-diamond crystal, not for gyroid or simple primitive crystals [27]. Fast Fourier Transforms (FFTs) of the TEM images and the matching computer-generated images yielded the lattice constant of the diamond crystal: $a = 445 \pm 10$ nm as well as the Miller indices of the orientation of the crystal. Miller indices ($h k l$) give the directions and planes of equal symmetry of a crystal with respect to the standard unit cell, i.e. the normal of the crystal orientation with respect to the scale surface [10].

Having derived the lattice constant, $a = 445$ nm, we subsequently calculated reflectance spectra for the differently-oriented, single-diamond photonic crystals. We used a parallel Maxwell solver and calculated the reflectance for TE-(Transverse Electric, or s-) as well as for TM-(Transverse Magnetic, or p-) polarized light (figure 3). The simulated reflectance spectra had a half-width (FWHM) ~30-80 nm and peaked in the blue to yellow-orange wavelength range, from 490 nm to 580 nm. For each orientation, given by the Miller indices in figure 3, the TE- and TM-reflectance spectra differed only very slightly in peak wavelength (~20 nm) and peak amplitude (~0.1). We therefore averaged the TE- and TM-reflectance spectra calculated for the various orientations of the crystal domains (figure 3). The experimental reflectance spectra of single domains, which were measured with unpolarized light (figure 1d), closely correspond to the averaged calculated spectra.

Effect of the scale arrangement on spatial visibility

The FDTD calculations predicted very directional, mirror-like reflections for the individual crystal orientations (see inset of figure 3). To determine the spatial reflection properties of the scales, and especially to assess how the scale arrangement in elytral pits affects the spatial scale reflection properties, we performed imaging scatterometry (ISM). For this we glued both single scales and small pieces of elytra with scale-carrying pits to the tip of pulled micropipettes and illuminated them with a narrow aperture, white light beam with a variable spot size.

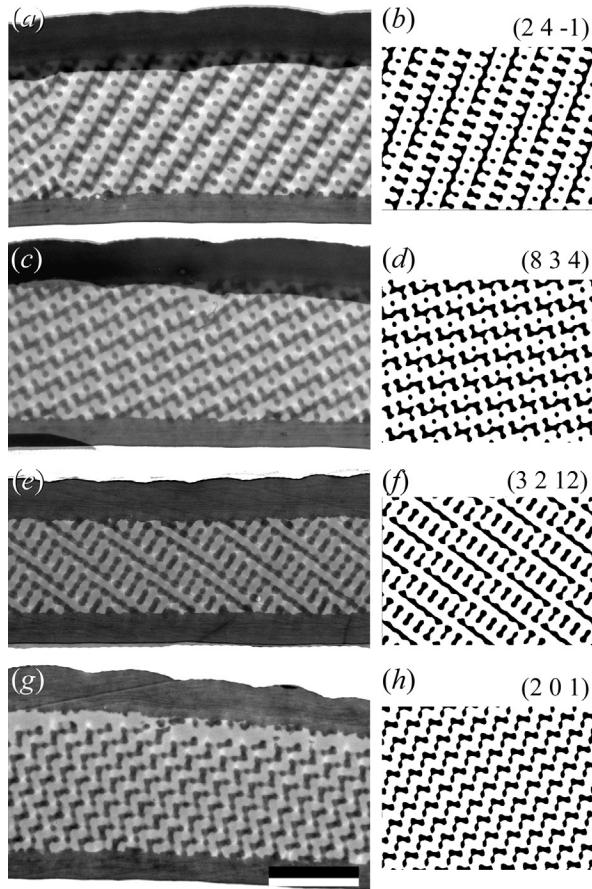


Figure 2. TEM of single scales revealing different orientations. The left column (*a, c, e, g*) shows a side-view of four different scales (bar: 2 μm , in *g*). The right column (*b, d, f, h*) shows the matching crystal orientations of a single diamond crystal with a chitin filling fraction ~ 0.3 and thickness $0.2a$ (a is the lattice constant). The orientations are given by the Miller indices ($h k l$) above each simulated cross-section.

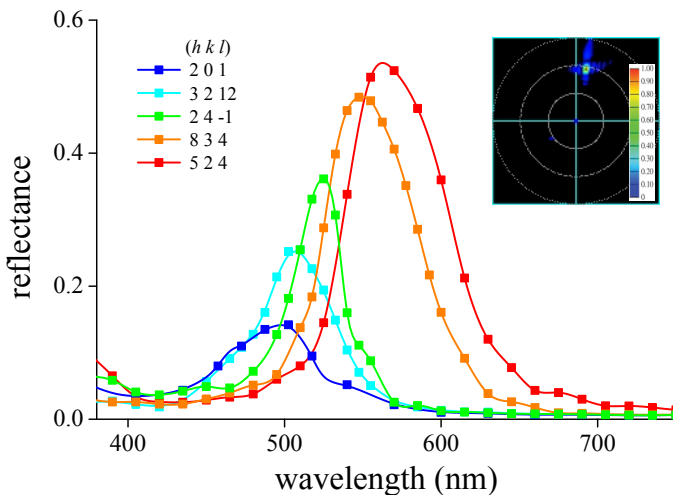


Figure 3. Reflectance spectra calculated with FDTD for a diamond-type photonic crystal with orientation denoted by the Miller indices ($h k l$) when exposed to unpolarised light. For this, spectra calculated for TE- and TM-polarised light were averaged. The lattice constant of the single diamond-type crystal was set to $a = 445$ nm. The inset shows the calculated scattering diagram for the $(8\ 3\ 4)$ -domain for normal-incident, TM-polarized light with wavelength 550 nm. The scattered light is concentrated in a very narrow spatial angle.

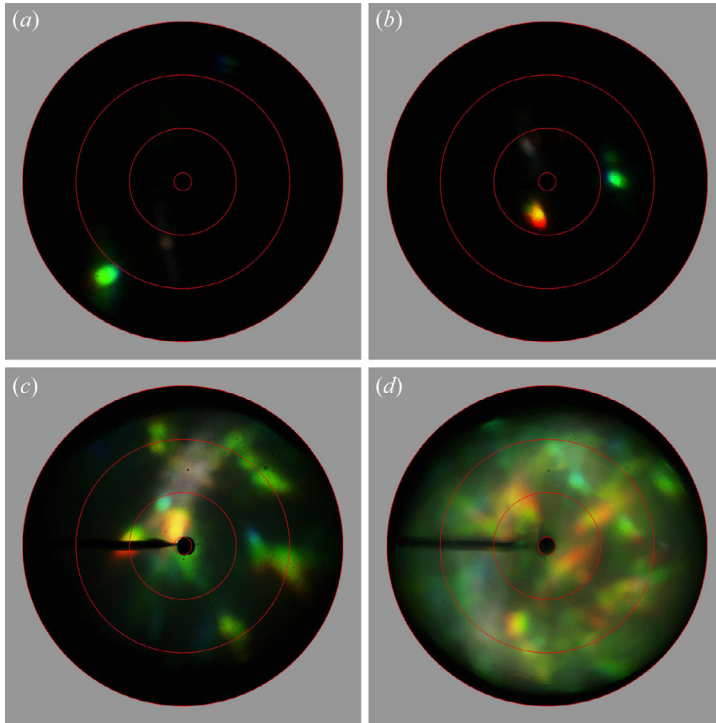


Figure 4. Imaging scatterometry of single domains, single scales and multiple scales illuminated with a narrow-aperture light beam ($\sim 5^\circ$). The illumination spot size was $15\ \mu\text{m}$ (a), $50\ \mu\text{m}$ (b), $140\ \mu\text{m}$ (c) and $800\ \mu\text{m}$ (d). (a) A single domain creates a scatter pattern with a very narrow-aperture of $\sim 5^\circ$. (b) Illumination of a single scale with two domains leads to two narrow reflection spots. (c) Illumination of four to five scales leads to a multitude of spots, or to a spatially extended scatter pattern, determined by the number of domains in the scale. (d) Illumination of all scales in one pit results in a scatter pattern that covers the whole hemisphere, with a number of distinct spots over a more or less uniform green-yellow background.

Figure 4 presents the scatterograms resulting from differently sized illumination areas; a single domain (spot size diameter $d = 15\ \mu\text{m}$; figure 4a), a single scale ($d = 50\ \mu\text{m}$; figure 4b), a few scales ($d = 140\ \mu\text{m}$; figure 4c), and the complete pit ($d = 800\ \mu\text{m}$; figure 4d). Illumination of single domains (figure 4a) resulted in light-scattering profiles with a distinct colour and a very narrow solid angle. The spatial extent of the reflected spots, half-width of $5\text{-}10^\circ$, was virtually identical to the aperture of the illumination beam, which was $\sim 5^\circ$ [33]. Strikingly, the angular position of the reflected spot severely differed between the domains, meaning that the directions of the reflected light beams severely deviated from each other (figure 4a; see also inset figure 3b for the simulated reflection pattern of a single domain).

Increasing the spot size increased the complexity of the reflection pattern. Illumination of only a restricted number of scales, each having a small number of different domains, caused a scatter pattern that was the sum of the directional reflections of the single domains (figure 4b,c). An increase in the size of the illuminated area increased the number of reflected spots in the scatterogram. When a whole elytral pit was illuminated, further broadening of the reflection pattern occurred (figure 4d). The scatterograms then contained a few prominent reflection spots on a more or less angle-independent green-yellow background.

Large-area reflections of the weevil elytra

Under normal circumstances light will be scattered by numerous elytral scales, not by single scales or single domains. The reflectance spectrum measured from a large area hence will be the weighted sum of the spectra of the illuminated individual domains with different orientations (figure 4). To assess the overall colour reflectance of the diamond weevil, we measured the reflectance spectrum of the elytra with an integrating sphere, which had a

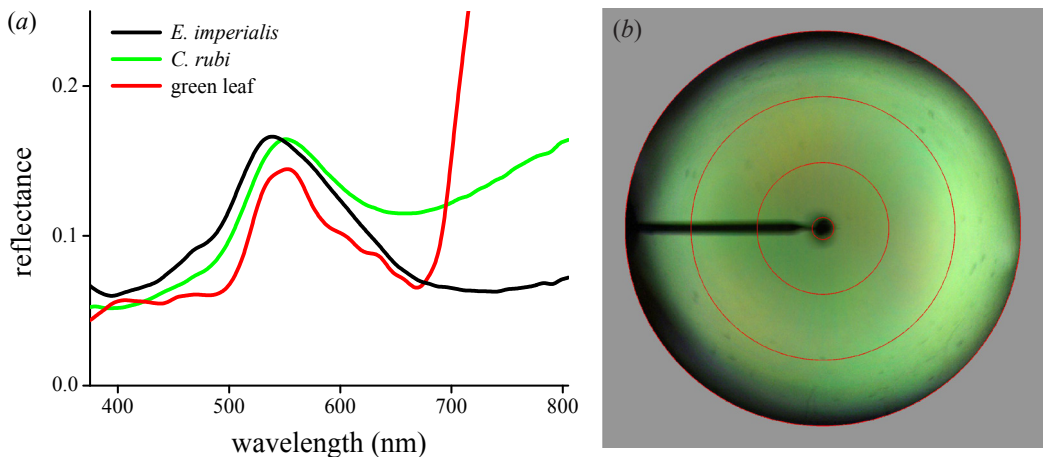


Figure 5. Brilliant camouflage. (a) Reflectance spectra measured with an integrating sphere of an elytron of the diamond weevil, *Entimus imperialis*, of a green oak leaf, and of the wing underside of the Green Hairstreak butterfly, *Callophrys rubi*. (b) Scatter pattern of a single scale-carrying pit in a weevil elytron illuminated with wide-aperture white light.

large illumination spot size, ~ 8 mm, thus capturing ~ 10 elytral pits. As expected, the resulting reflectance spectrum, peak wavelength ~ 540 nm and half-width ~ 180 nm, was considerably broader than the spectra of single domains (figure 5a). Interestingly, the reflectance spectrum of the large illumination spot strongly resembles the reflectance spectra of green leaves. Wide-angle illumination of a single pit also results in an approximately angle-independent green colouration (figure 5b).

DISCUSSION

Biophotonic structures in weevils and beetles

The elytral scales of the weevil *Entimus imperialis* have uniquely large domains, which allow spectral measurements on individual domains. Both the directionality of the reflected light and the measured reflectance spectra are in full agreement with predictions based on the derived anatomical data and the structure of diamond-type photonic crystals.

Photonic crystals with a diamond structure seem to be restricted to beetles and weevils (Coleoptera) [1], whereas photonic crystals with a gyroid structure have so far only been encountered in lycaenid and papilionid butterflies [6,25,27]. In nascent butterfly wing scales, specific interactions of the cell plasma membrane and the intracellular smooth endoplasmic reticulum initiate the development of single gyroid networks by cubic membrane folding via a double gyroid intermediate [27,37]. To date, relatively little is known about the development of nascent weevil wing scales. Concerning the diamond structures we may speculate that the developmental pathway involves a double diamond intermediate, as this intermediate is observed as a stable phase in cubic membrane folding [38,39]. The presence of diamond-type photonic crystals in weevil scales may have distinct evolutionary advantages that can range from differences in reflectance properties to enhancement of mating chances [5]. Light reflected by gyroid photonic crystals can be

highly polarized [28], whereas diamond photonic crystals show hardly any polarization dependency (see figure 3 and refs. [10,22,26]). Whether or not this difference in polarization properties has a biological function has yet to be investigated.

Biological implications of the scale arrangement

Single scale domains exhibit strong reflections in narrow spatial angles (figure 4a,b). The reflecting domains in the scale assembly in an elytral pit together create a distinct, vividly coloured spot. The distance between the elytral pits is ~ 1 mm, so that, assuming a spatial resolution of the weevil eyes of $\sim 1^\circ$ [40], potential mates can discriminate adjacent spots from a distance as far as ~ 6 cm. The near-field brilliancy of the dotted pattern of the weevil's elytra may therefore be used as a mate recognition signal [3].

The scales in a pit all have a similar orientation. Their tips are directed towards the elytral apex, corresponding to the general scale patterning of weevil elytra. However, the scales at the slopes of the conical pits have different angular orientations and this causes a spatially broadened reflection signal. The pit will therefore act effectively as a signal scrambler, by creating an overall multi-domain arrangement comparable to that observed in single scales of the weevil *L. augustus* [23] or the ventral wing scales of the Green Hairstreak butterfly, *Callophrys rubi* [6,27]; in these cases the domain size is smaller by a factor of about ten.

Overall, the array of coloured pits gives rise to a uniform, diffusely green-yellow appearance when illuminated with a wide-angled light source (figure 5b). The integral yellow-green reflectance closely mimics the reflectance of green leaves (generally leaf spectra resemble the spectrum of an oak leaf, shown as an example in figure 5b). This immediately suggests that the coloured scales in the concave pits serve to camouflage the weevil against a mainly green background (see also figure 1a), especially for their common predators, birds [40]. Further, the dotted arrangement of the pits on the elytra will support camouflage by disruptive patterning, a common mechanism to achieve camouflage [8], e.g. applied by cuttlefish [7, 41].

The coloured scales of *Entimus imperialis* are concentrated in concave pits on its black elytra. Clearly the scales are thus not vulnerable to mechanical wear. The concentration of the scales in pits therefore presumably serve three functions: the scales are protected from mechanical damage and accidental loss, the pattern of brilliant spots facilitates intraspecific recognition, and the integral green colouration favours camouflage in foliaceous environments [3,4].

REFERENCES

1. Seago, A. E., Brady, P., Vigneron, J. P. & Schultz, T. D. 2009 Gold bugs and beyond: a review of iridescence and structural colour mechanisms in beetles (Coleoptera). *J. R. Soc. Interface* **6 Suppl 2**, S165-S184.
2. Kinoshita, S. 2008 Structural colors in the realm of nature, Singapore: World Scientific.
3. Doucet, S. M. & Meadows, M. G. 2009 Iridescence: a functional perspective. *J. R. Soc. Interface* **6 Suppl 2**, S115-S132.
4. Meadows, M. G., Butler, M. W., Morehouse, N. I., Taylor, L. A., Toomey, M. B., McGraw, K. J. & Rutowski, R. L. 2009 Iridescence: views from many angles. *J. R. Soc. Interface* **6 Suppl 2**, S107-S113.
5. Darwin, C. 1859 The origin of species by means of natural selection, or the preservation of favoured races in the struggle for life. London, UK: John Murray.

6. Michielsen, K., De Raedt, H. & Stavenga, D. G. 2010 Reflectivity of the gyroid biophotonic crystals in the ventral wing scales of the Green Hairstreak butterfly, *Callophrys rubi*. *J. R. Soc. Interface* **7**, 765-771.
7. Buresch, K. C., Mähger, L. M., Allen, J. J., Bennice, C., Smith, N., Schram, J., Chiao, C. C., Chubb, C. & Hanlon, R. T. 2011 The use of background matching vs. masquerade for camouflage in cuttlefish *Sepia officinalis*. *Vision Res.* **51**, 2362-2368.
8. Stevens, M. & Merilaita, S. 2009 Defining disruptive coloration and distinguishing its functions. *Phil. Trans. R. Soc. B* **364**, 481-488.
9. Mähger, L. M. & Hanlon, R. T. 2007 Malleable skin coloration in cephalopods: selective reflectance, transmission and absorbance of light by chromatophores and iridophores. *Cell Tissue Res.* **329**, 179-186.
10. Joannopoulos, J. D. 2008 Photonic crystals: molding the flow of light, 2nd edn. Princeton: Princeton University Press.
11. Mähger, L. M., Land, M. F., Siebeck, U. E. & Marshall, N. J. 2003 Rapid colour changes in multilayer reflecting stripes in the Paradise Whiptail, *Pentapodus paradiseus*. *J. Exp. Biol.* **206**, 3607-3613.
12. Stavenga, D. G., Wilts, B. D., Leertouwer, H. L. & Hariyama, T. 2011 Polarized iridescence of the multilayered elytra of the Japanese Jewel Beetle, *Chrysochroa fulgidissima*. *Phil. Trans. R. Soc. B* **366**, 709-723.
13. Hariyama, T., Hironaka, M., Takaku, Y., Horiguchi, H. & Stavenga, D. G. 2005 The leaf beetle, the jewel beetle, and the damselfly; insects with a multilayered show case. In *Structural color in biological systems - principles and applications* (eds Kinoshita, S. & Yoshioka, S.), pp. 153-176. Osaka: Osaka University Press.
14. Mason, C. W. 1927 Structural colors in insects. III. *J. Phys. Chem.* **31**: 1856-1872.
15. Durrer, H. & Villiger, W. 1972 Schillerfarben von *Euchroma gigantea* (L.): (Coleoptera: Buprestidae): Elektronenmikroskopische Untersuchung der Elytra. *Int. J. Insect Morphol. Embryol.* **1**, 233-240.
16. Sharma, V., Crne, M., Park, J. O. & Srinivasarao, M. 2009 Structural Origin of Circularly Polarized Iridescence in Jeweled Beetles. *Science* **325**, 449-451.
17. Brady, P. & Cummings, M. 2010 Differential response to circularly polarized light by the jewel scarab beetle *Chrysina gloriosa*. *Am. Nat.* **175**, 614-620.
18. Stavenga, D. G., Leertouwer, H. L., Marshall, N. J. & Osorio, D. 2011 Dramatic colour changes in a bird of paradise caused by uniquely structured breast feather barbules. *Proc. R. Soc. B* **278**, 2098-2104.
19. Zi, J., Yu, X., Li, Y., Hu, X., Xu, C., Wang, X., Liu, X. & Fu, R. 2003 Coloration strategies in peacock feathers. *Proc. Natl. Acad. Sci. USA* **100**, 12576-12578.
20. Loyau, A., Gomez, D., Moureau, B., Thery, M., Hart, N. S., Saint Jalme, M., Bennett, A. T. D. & Sorci, G. 2007 Iridescent structurally based coloration of eyespots correlates with mating success in the peacock. *Behav. Ecol.* **18**, 1123-1131.
21. Parker, A. R., Welch, V. L., Driver, D. & Martini, N. 2003 Structural colour: opal analogue discovered in a weevil. *Nature* **426**, 786-787.
22. Wilts, B. D., Michielsen, K., De Raedt, H. & Stavenga, D. G. 2012 Hemispherical Brillouin zone imaging of a diamond-type biological photonic crystal. *J. R. Soc. Interface* **9**, 1609-1614.
23. Galusha, J. W., Richey, L. R., Gardner, J. S., Cha, J. N. & Bartl, M. H. 2008 Discovery of a diamond-based photonic crystal structure in beetle scales. *Phys. Rev. E* **77**, 050904.
24. Welch, V., Lousse, V., Deparis, O., Parker, A. & Vigneron, J. P. 2007 Orange reflection from a three-dimensional photonic crystal in the scales of the weevil *Pachyrrhynchus congestus pavonius* (Curculionidae). *Phys. Rev. E* **75**, 041919.
25. Michielsen, K. & Stavenga, D. G. 2008 Gyroid cuticular structures in butterfly wing scales: biological photonic crystals. *J. R. Soc. Interface* **5**, 85-94.
26. Poladian, L., Wickham, S., Lee, K. & Large, M. C. 2009 Iridescence from photonic crystals and its suppression in butterfly scales. *J. R. Soc. Interface* **6 Suppl 2**, S233-S242.
27. Saranathan, V., Osuji, C. O., Mochrie, S. G., Noh, H., Narayanan, S., Sandy, A., Dufresne, E. R. & Prum, R. O. 2010 Structure, function, and self-assembly of single network gyroid (I4132) photonic crystals in butterfly wing scales. *Proc. Natl. Acad. Sci. USA* **107**, 11676-11681.
28. Saba, M., Thiel, M., Turner, M. D., Hyde, S. T., Gu, M., Grosse-Brauckmann, K., Neshev, D. N., Mecke, K. & Schröder-Turk, G. E. 2011 Circular dichroism in biological photonic crystals and cubic chiral nets. *Phys. Rev. Lett.* **106**, 103902.
29. Shawkey, M. D., Saranathan, V., Palsdottir, H., Crum, J., Ellisman, M. H., Auer, M. & Prum, R. O. 2009 Electron tomography, three-dimensional Fourier analysis and colour prediction of a three-dimensional amorphous biophotonic nanostructure. *J. R. Soc. Interface* **6 Suppl 2**, S213-S220.
30. Dong, B. Q., Liu, X. H., Zhan, T. R., Jiang, L. P., Yin, H. W., Liu, F. & Zi, J. 2010 Structural coloration and photonic pseudogap in natural random close-packing photonic structures. *Opt. Express* **18**, 14430-14438.

31. Morrone, J. J. 2002 The Neotropical weevil genus *Entimus* (Coleoptera : Curculionidae : Entiminae): Cladistics, biogeography, and modes of speciation. *Coleopt. Bull.* **56**, 501-513.
32. Mc Kay, F., Oleiro, M., Cabrera Walsh, G., Gandolfo, D., Cuda, J. P. & Wheeler, G. S. 2009 Natural enemies of Brazilian Peppertree (Sapindales: Anacardiaceae) from Argentina: their possible use for biological control in the USA. *Fla. Entomol.* **92**, 292-303.
33. Stavenga, D. G., Leertouwer, H. L., Pirihi, P. & Wehling, M. F. 2009 Imaging scatterometry of butterfly wing scales. *Opt. Express* **17**, 193-202.
34. Vukusic, P. & Stavenga, D. G. 2009 Physical methods for investigating structural colours in biological systems. *J. R. Soc. Interface* **6 Suppl 2**, S133-S148.
35. Vukusic, P., Sambles, J. R., Lawrence, C. R. & Wootton, R. J. 1999 Quantified interference and diffraction in single Morpho butterfly scales. *Proc. R. Soc. B* **266**, 1403-1411.
36. Leertouwer, H. L., Wilts, B. D. & Stavenga, D. G. 2011 Refractive index and dispersion of butterfly chitin and bird keratin measured by polarizing interference microscopy. *Opt. Express* **19**, 24061-24066.
37. Ghiradella, H. 1989 Structure and development of iridescent butterfly scales: Lattices and laminae. *J. Morphol.* **202**, 69-88.
38. Hyde, S., Andersson, S., Larsson, K., Blum, Z., Landh, T., Lidin, S. & Ninham, B. 1997 The Language of shape: the role of curvature in condensed matter: physics, chemistry, and biology, Amsterdam: Elsevier.
39. Almsharqi, Z. A., Kohlwein, S. D. & Deng, Y. 2006 Cubic membranes: a legend beyond the Flatland of cell membrane organization. *J. Cell Biol.* **173**, 839-844.
40. Osorio, D. & Vorobyev, M. 2005 Photoreceptor spectral sensitivities in terrestrial animals: adaptations for luminance and colour vision. *Proc. R. Soc. B* **272**, 1745-1752.
41. Cuthill, I. C., Stevens, M., Sheppard, J., Maddocks, T., Parraga, C. A. & Troscianko, T. S. 2005 Disruptive coloration and background pattern matching. *Nature* **434**, 72-74.

